

Singlino Resonant Dark Matter and 125 GeV Higgs Boson in High-Scale Supersymmetry

Kazuya Ishikawa,^{*} Tepei Kitahara,[†] and Masahiro Takimoto[‡]

Department of Physics, Faculty of Science, University of Tokyo, Bunkyo-ku, Tokyo 113-0033, Japan

(Received 6 June 2014; published 23 September 2014)

We consider a singlino dark matter (DM) scenario in a singlet extension model of the minimal supersymmetric standard model, which is the so-called the nearly minimal supersymmetric standard model. We find that with high-scale supersymmetry breaking the singlino can obtain a sizable radiative correction to the mass, which opens a window for the DM scenario with resonant annihilation via the exchange of the Higgs boson. We show that the current DM relic abundance and the Higgs boson mass can be explained simultaneously. This scenario can be fully probed by XENON1T.

DOI: 10.1103/PhysRevLett.113.131801

PACS numbers: 12.60.Jv, 12.60.Fr, 14.80.Da, 95.35.+d

The supersymmetric (SUSY) models are good candidates of the physics beyond the standard model (SM), because they solve the hierarchy problem and ensure the unification of the gauge couplings. In addition, the lightest SUSY particle (LSP) can be a natural candidate of the dark matter (DM) if the R parity is conserved. However, the minimal SUSY extension of the SM (MSSM) contains a dimensionful parameter μ , and it causes the “ μ problem” [1]. Although μ must be the size of the SUSY breaking scale to realize the electroweak symmetry breaking properly, there is no reason for μ to be small compared to the Planck scale. One of the simplest ways to solve this problem is to introduce a gauge-singlet superfield. There are several models of singlet extension of the MSSM depending on the imposed symmetry (for a review, see [2]). The nearly minimal (or new minimal) supersymmetric standard model (nMSSM) [3–5] based on \mathbb{Z}_5^R or \mathbb{Z}_7^R R symmetry does not suffer from the domain wall problem, unlike \mathbb{Z}_3 symmetric models (NMSSM) [6,7]. Therefore, the nMSSM is one of the promising models of the new physics.

On the other hand, recent various cosmological observations have established the Λ CDM cosmological model, and the relic abundance of the cold DM is measured accurately [8,9]. In the nMSSM, the singlino can be a candidate of the DM [5,10–14]. But they seem to be incompatible with relatively high-scale (TeV-scale) supersymmetry breaking, which is inferred from the measured SM Higgs boson mass [15,16] and the null results of the sparticle searches at the Large Hadron Collider (LHC) [17,18]. This is because the singlino mass and its couplings with SM particles have been thought to be suppressed by the SUSY breaking scale, which leads to overabundant singlino DM in the Universe. However, if one-loop corrections to the singlino mass are taken into account, the singlino can obtain a sizable mass, which opens a window for a resonant DM scenario via the s -channel annihilation with the exchange of the SM Higgs boson. Furthermore, in these resonant DM scenarios, since the annihilation rate of the singlino is p -wave suppressed, one

needs a relatively large value of the Higgs-DM coupling. This fact implies that the singlino DM can be probed more readily than the scalar one [19].

In this Letter, we study the singlino resonant DM scenario within the high-scale nMSSM including one-loop corrections to the neutralino masses. We will show that if the SUSY breaking scale is around ~ 10 TeV and $\tan\beta$ is relatively low, the current DM abundance and the measured SM Higgs boson mass can be achieved simultaneously. We will also find that this scenario can be fully probed by the proposed future DM search XENON1T [20].

This Letter is organized as following. In the next section, we give a short review of the nMSSM. We present properties of the singlino in the following section. In the third section, we investigate the singlino resonant DM scenario with high-scale SUSY breaking, which is compatible with the SM Higgs boson mass ~ 125 GeV. The last section is devoted to the conclusion and discussions.

The nearly MSSM.—In this section, we briefly review the nMSSM [3–5].

In the nMSSM, to solve the μ problem a gauge-singlet chiral superfield \hat{S} is introduced. The superpotential and the soft SUSY breaking terms are given as

$$W = \lambda \hat{S} \hat{H}_u \cdot \hat{H}_d + \frac{m_{12}^2}{\lambda} \hat{S} + W_{\text{Yukawa}}, \quad (1)$$

$$V_{\text{soft}} = m_{\hat{S}}^2 |S|^2 + (\lambda A_\lambda H_u \cdot H_d S + t_S S + \text{H.c.}) + V_{\text{soft}}^{\text{MSSM}}, \quad (2)$$

where \hat{H}_u (\hat{H}_d) is the up (down)-type Higgs doublet superfield. Although the terms m_{12}^2 and t_S are forbidden by a discrete \mathbb{Z}_5^R (\mathbb{Z}_7^R) R symmetry when supersymmetry is conserved, they are generated by supergravity effects as

$$m_{12}^2 = \lambda \xi_F M_{\hat{S}}^2, \quad (3)$$

$$t_S = \xi_S M_{\hat{S}}^3, \quad (4)$$

where M_S denotes the SUSY breaking scale (see Refs. [3–5]). Here ξ_F and ξ_S are $\mathcal{O}(1)$ constants, and then m_{12}^2 and t_S become $\mathcal{O}(M_S^2)$ and $\mathcal{O}(M_S^3)$, respectively [21]. With these values, S has a vacuum expectation value $\langle S \rangle \sim -t_S/m_S^2 \sim \mathcal{O}(M_S)$. This vacuum expectation value generates an effective μ parameter $\mu_{\text{eff}} \equiv \lambda \langle S \rangle \sim \mathcal{O}(M_S)$, and the μ problem is solved.

At the tree level, the neutralino mass matrix in the basis $(\tilde{B}, \tilde{W}^0, \tilde{H}_d^0, \tilde{H}_u^0, \tilde{S})$ is

$$\mathcal{M}_{\text{tree}} = \begin{pmatrix} M_1 & 0 & -\frac{g_1 v_d}{\sqrt{2}} & \frac{g_1 v_u}{\sqrt{2}} & 0 \\ & M_2 & \frac{g_2 v_d}{\sqrt{2}} & -\frac{g_2 v_u}{\sqrt{2}} & 0 \\ & & 0 & -\mu_{\text{eff}} & -\lambda v_u \\ & & & 0 & -\lambda v_d \\ & & & & 0 \end{pmatrix}, \quad (5)$$

where \tilde{B} is the bino, \tilde{W}^0 is the neutral wino, \tilde{H}_d^0 and \tilde{H}_u^0 are the neutral Higgsinos, and \tilde{S} is the fermionic component of \hat{S} . v_u (v_d) is the vacuum expectation value of H_u^0 (H_d^0) with $v^2 \equiv v_u^2 + v_d^2 \approx (174 \text{ GeV})^2$. M_1 and M_2 are the gaugino masses, where the gauge couplings for $U(1)_Y$ and $SU(2)$ are denoted as g_1 and g_2 , respectively. We denote \tilde{s} as the mass-eigenstate neutralino whose component is mainly \tilde{S} . We call \tilde{s} a singlino in this Letter. When the SUSY breaking scale is relatively high as suggested by the LHC experiments [15–18], the singlino becomes the LSP and it can be a good candidate of the DM.

In the nMSSM, since the SM Higgs boson has an extra contribution to the quartic coupling λ_{quartic} , there is a sizable tree-level contribution to the Higgs boson mass. When integrating out heavy SUSY particles and matching with the SM, the SM Higgs quartic coupling is shifted by [22]

$$\delta\lambda_{\text{quartic}} = \frac{\lambda^2 m_S^2 - A_\lambda^2}{2 m_S^2} \sin^2 2\beta, \quad (6)$$

compared to the MSSM. Large λ and small $\tan\beta$ can give a sizable contribution to the Higgs boson mass. However, note that this extra contribution becomes small if $m_S \sim A_\lambda$.

DM abundance and radiative singlino mass in the nMSSM.—In this section, we calculate the DM abundance and briefly estimate the singlino mass in the nMSSM.

Let us consider the case where only the singlino \tilde{s} is light and other SUSY particles are relatively heavy. In this case, the low-energy effective Lagrangian can be written as

$$-\mathcal{L}_{\text{eff}} \supset \frac{m_{\tilde{s}}}{2} \tilde{s} \tilde{s} + \frac{\lambda_{\text{eff}}}{2} h \tilde{s} \tilde{s}, \quad (7)$$

where h corresponds to the SM Higgs boson. Before going to the numerical calculation in the nMSSM, we estimate the thermal relic abundance of singlino with this effective

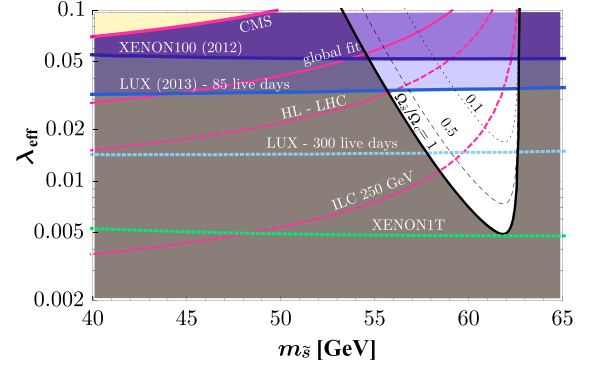


FIG. 1 (color online). The singlino thermal relic abundance and experimental constraints or future prospects. The black lines denote the ratio of the thermal relic abundance $\Omega_{\tilde{s}} h^2$ to the current DM density $\Omega_c h^2 = 0.1199$ [9]. The singlino relic density overcloses the Universe at the dark-shaded region. The regions above the red solid lines are excluded by the Higgs invisible decay ($h \rightarrow \tilde{s} \tilde{s}$) searches of CMS ($\text{Br}_h^{\text{inv}} \leq 58\%$) [24] for the upper line (yellow-shaded region) and by the global fit of the Higgs couplings (19%) [25] for the lower line. The dashed red lines correspond to the future sensitivity of high luminosity LHC (6.2%) [26] and ILC with $\mathcal{L} = 1150 \text{ fb}^{-1}$ at $\sqrt{s} = 250 \text{ GeV}$ (0.4%) [27]. The blue-shaded regions are excluded by XENON100 [28] and LUX [29]. The regions above the blue and the green dashed lines can be probed by the future direct DM searches of LUX [30] and XENON1T [20].

model regarding λ_{eff} and $m_{\tilde{s}}$ as free parameters by solving the Boltzmann equation [23]. In Fig. 1, the black lines show the ratio of the thermal relic abundance $\Omega_{\tilde{s}} h^2$ to the current DM density $\Omega_c h^2 = 0.1199$ [9], where we take the Higgs boson mass as $m_h = 125.5 \text{ GeV}$. The regions above the red solid lines are excluded by the Higgs invisible decay ($h \rightarrow \tilde{s} \tilde{s}$) searches of CMS (upper line) [24] and by the global fit of the Higgs couplings (lower line) [25]. The regions above the red dashed lines can be probed by the future Higgs invisible decay searches of high luminosity LHC (upper line) [26] and ILC (lower line) [27]. The direct DM searches set limits on the spin-independent cross section of DM-nucleon elastic scattering. The blue-shaded regions are excluded by the direct DM searches of XENON100 [28] and LUX [29]. The region above the blue (green) dashed line can be probed by the future direct DM search of LUX [30] (XENON1 T [20]). For applying these constraints and future prospects, we assume $\Omega_{\tilde{s}} h^2 = \Omega_c h^2$. The gray-shaded region is excluded by the overclosure of the Universe. One can see that the region where \tilde{s} is consistent with the current DM relic abundance lies around $\lambda_{\text{eff}} \sim \mathcal{O}(0.01)$ and $m_{\tilde{s}} \sim 60 \text{ GeV}$. In this region, resonant pair annihilation of \tilde{s} occurs via the Higgs boson with $m_{\tilde{s}} \sim m_h/2$. This allowed region can be covered by the future Higgs invisible decay searches and direct DM searches, especially by XENON1T.

Now, we estimate $m_{\tilde{s}}$ and λ_{eff} in the nMSSM. From the tree-level calculations, these values are evaluated as

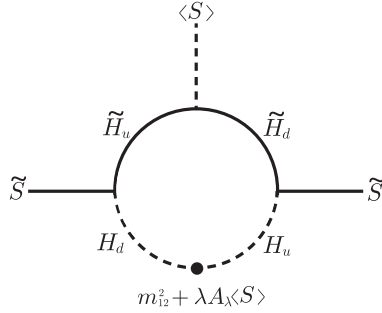


FIG. 2. Typical one-loop diagram which contributes to the singlino mass.

$$m_{\tilde{s}}^{\text{tree}} \sim \lambda^2 \frac{v^2}{M_S} \sin 2\beta, \quad (8)$$

$$\lambda_{\text{eff}}^{\text{tree}} \sim \lambda^2 \frac{v}{M_S} \sin 2\beta, \quad (9)$$

where $\tan\beta \equiv v_u/v_d$ and we denote the typical SUSY breaking scale by M_S . Obviously, $\lambda_{\text{eff}} \sim \mathcal{O}(0.01)$ and $m_{\tilde{s}} \sim 60$ GeV cannot be satisfied at the same time. However, one-loop corrections to the neutralino mass [31] can raise the singlino mass with relatively large M_S . The typical diagram which contributes to the singlino mass is given in Fig. 2. The one-loop singlino mass can be estimated as

$$\begin{aligned} m_{\tilde{s}}^{\text{1-loop}} &\sim \frac{\lambda^2}{(4\pi)^2} \mu_{\text{eff}} \sin 2\beta F \left(\frac{2(m_{12}^2 + A_\lambda \mu_{\text{eff}})}{\mu_{\text{eff}}^2 \sin 2\beta} \right) \\ &\sim \frac{\lambda^2}{(4\pi)^2} M_S \sin 2\beta, \end{aligned} \quad (10)$$

where the loop function $F(x)$ is defined as $F(x) \equiv (x \log x)/(x-1)$ and satisfies $F(1) = 1$. We calculate the singlino mass including the full one-loop corrections [31,32]. Figure 3 shows the dependence of M_S to the singlino mass in the tree level and the one-loop level. In this

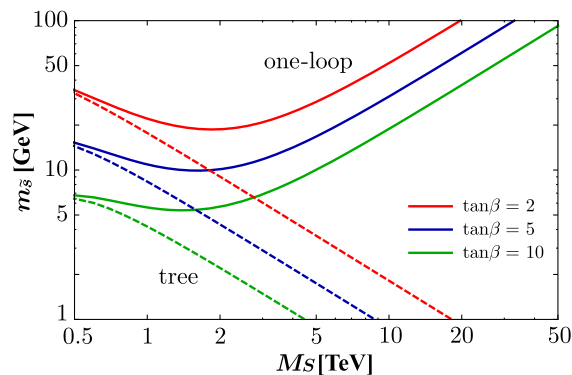


FIG. 3 (color online). The one-loop-level singlino mass and the tree-level one as a function of M_S .

figure, we take $\lambda = 0.75$ and all dimensionful parameters equal to M_S . One can see that the singlino obtains sizable one-loop corrections to the mass in the high-scale SUSY scenario. Since this feature is due to the suppression of the singlino mass at the tree level, the two-loop-level correction to the singlino mass is estimated to be smaller than the one-loop one. Note that with $M_S \sim \mathcal{O}(10)$ TeV, $\tan\beta \sim \mathcal{O}(1)$, and $\lambda \sim \mathcal{O}(1)$, one can simply obtain $\lambda_{\text{eff}} \sim \mathcal{O}(0.01)$ and $m_{\tilde{s}} \sim 60$ GeV [34]. Moreover, the Higgs boson mass becomes around 125 GeV in such parameter sets with the help of the additional quartic coupling λ . We show the validity by using the numerical calculations in the next section.

Numerical results.—In this section, we numerically investigate the singlino resonant DM scenario and the Higgs boson mass in the nMSSM. In this Letter, we calculate the Higgs boson mass using the two-loop renormalization group equation including the matching condition (6) [22].

In Fig. 4, we show the singlino mass $m_{\tilde{s}}$ (red lines), the effective Higgs-DM coupling λ_{eff} (blue lines), and the Higgs boson mass m_h (black dashed lines) in the M_S - $\tan\beta$ plane. For simplicity, all parameters are chosen to be real. The trilinear coupling λ is taken to be λ_{max} , which is a maximal value avoiding Landau singularities up to the grand unified theory scale, 2×10^{16} GeV. All SUSY breaking parameters except A_λ are set to M_S ($\lambda \xi_F = \xi_S = 1$). In order to obtain a sizable contribution to the Higgs boson mass, we choose $A_\lambda^2 = \frac{2}{5} M_S^2$. As one can see from Fig. 1, the viable regions for the singlino DM are $55.5 \text{ GeV} < m_{\tilde{s}} < 62.7 \text{ GeV}$ and $0.005 < \lambda_{\text{eff}} < 0.034$. In Fig. 4, these regions correspond to the red-shaded band

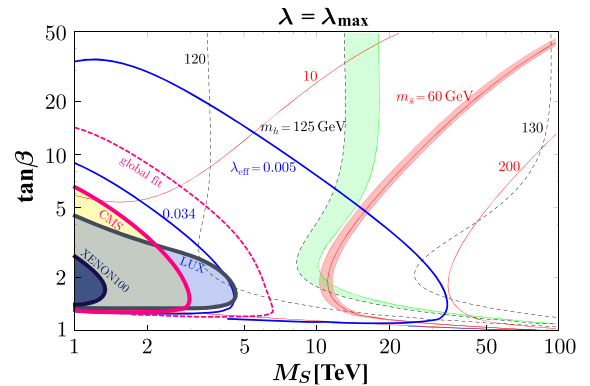


FIG. 4 (color online). Contours of $m_{\tilde{s}}$ (red lines), λ_{eff} (blue lines), and m_h (black dashed lines) in the M_S - $\tan\beta$ plane assuming $\lambda = \lambda_{\text{max}}$ at each point. On the red-shaded region ($55.5 \text{ GeV} < m_{\tilde{s}} < 62.7 \text{ GeV}$), the resonant annihilation via the Higgs boson can occur. The green-shaded region satisfies $125 \text{ GeV} < m_h < 126 \text{ GeV}$. The blue (dark blue)-shaded region is excluded by the current limits from LUX [29] (XENON [28]). The yellow-shaded region is excluded by the Higgs invisible decay search at the CMS [24], and the magenta dashed line is the current bound by the global fit of the Higgs couplings [25].

and the region between the two blue lines, respectively. The green band represents $125 \text{ GeV} < m_h < 126 \text{ GeV}$. One can see that the singlino resonant DM scenario is successful with $\tan\beta \sim \mathcal{O}(1)$ and $M_S \sim \mathcal{O}(10)$ TeV.

If we choose the lower value of A_λ^2 , the green line moves to the left, because the Higgs boson mass obtains more contribution from the quartic coupling [see Eq. (6)]. On the other hand, with a smaller value of $m_{12}^2 + \lambda A_\lambda \langle S \rangle$ the singlino mass becomes lighter and the red-shaded region moves to the right. The blue lines are not sensitive to the choice of m_{12}^2 and A_λ , because λ_{eff} is determined by the SUSY breaking scale and $\tan\beta$. The important point is that in any case with $M_S \sim \mathcal{O}(10)$ TeV and low $\tan\beta$ the current DM abundance and the measured Higgs boson mass can be realized simultaneously. This opens a window for the singlino DM in high-scale supersymmetry.

Finally, we show these regions in detail (see Fig. 5). In this figure, the Higgs boson mass is fixed to be 125.5 GeV by changing λ , $0 \leq \lambda \leq \lambda_{\text{max}}$. The input parameters are the same as Fig. 4 except λ . In the dark-shaded regions, one cannot explain $m_h = 125.5 \text{ GeV}$. The singlino relic abundance $\Omega_{\tilde{s}} h^2$ is consistent with the current value on the purple line, $\Omega_c h^2 = 0.1199$ [9]. In the light blue region, $\Omega_{\tilde{s}} h^2 \leq \Omega_c h^2$. The left side of the dashed lines can be covered by LUX (blue) [30], XENON1 T (green) [20], and ILC (magenta) [27]. From this result, the future experiments can probe a sign of the singlino DM.

Conclusion and discussions.—In this Letter, we have studied the singlino resonant DM scenario within the high-scale nMSSM. By including one-loop corrections to the neutralino masses, the singlino can explain the current DM relic abundance through the resonant annihilation via the Higgs boson. We have shown that with high-scale SUSY breaking ~ 10 TeV and low $\tan\beta$, the DM relic abundance

and the SM Higgs boson mass can be explained simultaneously in this scenario. Even for the high-scale SUSY, we have also shown that the parameter region where the singlino DM is consistent with the current DM relic abundance can be fully probed by future experiments (see Figs. 1 and 5). Therefore, the singlino DM signal can be “a first sign” of the high-scale supersymmetry.

In this Letter, we have concentrated on the scenario of singlino DM with resonant annihilation via the Higgs boson. Now, let us consider other scenarios of the high-scale nMSSM. After integrating out heavy SUSY particles, in the effective theory there are SM particles and only one additional particle, the singlino. The singlino has interactions with the SM Higgs boson and with the Z boson. While the effective coupling with the Higgs boson is suppressed by v/M_S , the coupling with the Z boson is more suppressed by $\sim (v/M_S)^2$, which prevents the resonant scenario with the Z boson. In order for the singlino not to be overabundant, the resonant scenario with the SM Higgs boson is the last resort for the high-scale nMSSM.

The NMSSM is another model of the singlet extension of MSSM [2]. The superpotential is given as

$$W_{\text{NMSSM}} = \lambda \hat{S} \hat{H}_u \cdot \hat{H}_d + \frac{\kappa}{3} \hat{S}^3 + W_{\text{Yukawa}}. \quad (11)$$

In the NMSSM, the singlino can obtain a radiative correction to the mass in addition to the tree-level mass $m_{\tilde{s}}^{\text{tree}} \sim 2\kappa \langle S \rangle$. The singlino resonant DM scenario may be successful with small $\tan\beta$ and small κ in the high-scale SUSY scenario. In the small κ limit, a singletlike CP -odd scalar boson a becomes a pseudo-Nambu-Goldstone boson because of the existence of the global U(1) Peccei-Quinn symmetry. Therefore, one may be able to make a distinction between the singlino resonant scenario in the nMSSM and NMSSM by the search for $h \rightarrow aa$ [35].

Since there are some new sources of CP -violating phases in the nMSSM, the electric dipole moments (EDM) are generally generated through a relative phase between μ_{eff} and M_{gaugino} at the one-loop level. The electron EDM is roughly evaluated as

$$\begin{aligned} \left| \frac{d_e}{e} \right| &\sim \frac{5g_2^2 + g_1^2}{384\pi^2} \frac{m_e}{M_S^2} \sin\phi \tan\beta \text{ [GeV}^{-1}\text{]} \\ &\sim 6 \times 10^{-29} \left(\frac{10 \text{ TeV}}{M_S} \right)^2 \sin\phi \tan\beta \text{ [cm]}, \end{aligned} \quad (12)$$

where $\phi = \arg(\mu_{\text{eff}} M_{\text{gaugino}})$. One can obtain $|d_e| \sim \mathcal{O}(10^{-29}) \text{ ecm}$ with $\tan\beta \sim \mathcal{O}(1)$, $M_S \sim \mathcal{O}(10)$ TeV, and $\sin\phi \sim \mathcal{O}(1)$. Interestingly, the electron EDM of this size does not conflict with the current bound [36] and can be probed by some future experiments [37–39].

The authors thank Florian Staub for providing the fixed one-loop correction sets of the NMSSM. They are also grateful to Motoi Endo and Kazunori Nakayama for useful

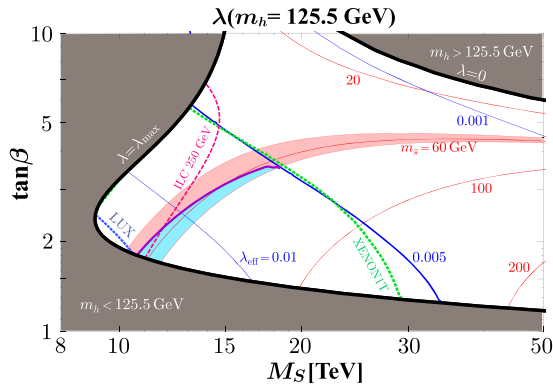


FIG. 5 (color online). Contours of $m_{\tilde{s}}$ (red lines) and λ_{eff} (blue lines) in the M_S - $\tan\beta$ plane under $m_h = 125.5 \text{ GeV}$ by changing λ , $0 \leq \lambda \leq \lambda_{\text{max}}$. On the purple line, the singlino relic abundance $\Omega_{\tilde{s}} h^2$ is consistent with the current value $\Omega_c h^2 = 0.1199$ [9]. In the light blue region, $\Omega_{\tilde{s}} h^2 \leq \Omega_c h^2$. The left side of the blue (green) dashed line can be probed by the future DM search LUX [30] (XENON1 T [20]). The ILC [27] can cover the left side of the magenta dashed line. Other lines are the same as in Fig. 4.

comments and discussions. The work of M. T. is supported in part by JSPS Research Fellowships for Young Scientists. The work of M. T. is also supported by the program for Leading Graduate Schools, MEXT, Japan.

*ishikawa@hep-th.phys.s.u-tokyo.ac.jp

†kitahara@hep-th.phys.s.u-tokyo.ac.jp

‡takimoto@hep-th.phys.s.u-tokyo.ac.jp

- [1] J. E. Kim and H. P. Nilles, *Phys. Lett.* **138B**, 150 (1984).
 [2] U. Ellwanger, C. Hugonie, and A. M. Teixeira, *Phys. Rep.* **496**, 1 (2010).
 [3] C. Panagiotakopoulos and K. Tamvakis, *Phys. Lett. B* **469**, 145 (1999).
 [4] C. Panagiotakopoulos and A. Pilaftsis, *Phys. Rev. D* **63**, 055003 (2001).
 [5] A. Dedes, C. Hugonie, S. Moretti, and K. Tamvakis, *Phys. Rev. D* **63**, 055009 (2001).
 [6] S. Abel, S. Sarkar, and P. White, *Nucl. Phys.* **B454**, 663 (1995).
 [7] C. Panagiotakopoulos and K. Tamvakis, *Phys. Lett. B* **446**, 224 (1999).
 [8] G. Hinshaw *et al.* (WMAP Collaboration), *Astrophys. J. Suppl. Ser.* **208**, 19 (2013).
 [9] P. Ade *et al.* (Planck Collaboration), [arXiv:1303.5076](https://arxiv.org/abs/1303.5076) [*Astron. Astrophys.* (to be published)].
 [10] A. Menon, D. Morrissey, and C. Wagner, *Phys. Rev. D* **70**, 035005 (2004).
 [11] V. Barger, P. Langacker, and H.-S. Lee, *Phys. Lett. B* **630**, 85 (2005).
 [12] C. Balazs, M. S. Carena, A. Freitas, and C. Wagner, *J. High Energy Phys.* **06** (2007) 066.
 [13] J. Cao, H. E. Logan, and J. M. Yang, *Phys. Rev. D* **79**, 091701 (2009).
 [14] W. Wang, *Adv. High Energy Phys.* **2012**, 22 (2012).
 [15] ATLAS Collaboration, Report No. ATLAS-CONF-2013-014, 2013; Report No. ATLAS-COM-CONF-2013-025, 2013.
 [16] CMS Collaboration, Report No. CMS-PAS-HIG-13-005, 2013.
 [17] ATLAS Collaboration, Report No. ATLAS-CONF-2013-047, 2013; Report No. ATLAS-COM-CONF-2013-049, 2013.
 [18] CMS Collaboration, Report No. CMS-PAS-SUS-13-004, 2013.
 [19] S. Kanemura, S. Matsumoto, T. Nabeshima, and N. Okada, *Phys. Rev. D* **82**, 055026 (2010).
 [20] E. Aprile (XENON1T Collaboration), *Springer Proc. Phys.* **148**, 93 (2013).
 [21] Although the trilinear κS^3 term is also generated, it is highly suppressed by the Planck scale.
 [22] G. F. Giudice and A. Strumia, *Nucl. Phys.* **B858**, 63 (2012).
 [23] P. Gondolo and G. Gelmini, *Nucl. Phys.* **B360**, 145 (1991).
 [24] S. Chatrchyan *et al.* (CMS Collaboration), *Eur. Phys. J. C* **74**, 2980 (2014).
 [25] G. Belanger, B. Dumont, U. Ellwanger, J. Gunion, and S. Kraml, *Phys. Rev. D* **88**, 075008 (2013).
 [26] S. Dawson *et al.*, [arXiv:1310.8361](https://arxiv.org/abs/1310.8361).
 [27] D. Asner *et al.*, [arXiv:1310.0763](https://arxiv.org/abs/1310.0763).
 [28] E. Aprile *et al.* (XENON100 Collaboration), *Phys. Rev. Lett.* **109**, 181301 (2012).
 [29] D. Akerib *et al.* (LUX Collaboration), *Phys. Rev. Lett.* **112**, 091303 (2014).
 [30] D. Akerib *et al.* (LUX Collaboration), *Nucl. Instrum. Methods Phys. Res., Sect. A* **704**, 111 (2013).
 [31] F. Staub, W. Porod, and B. Herrmann, *J. High Energy Phys.* **10** (2010) 040.
 [32] In the limit of $\kappa = 0$, one-loop corrections in the NMSSM reduce to the one in the mSSM. We found that Ref. [31] includes some typos in the equations of the one-loop corrections [33].
 [33] F. Staub (private communication).
 [34] The one-loop λ_{eff} can be roughly estimated as $\lambda_{\text{eff}}^{1\text{-loop}} \sim (\lambda^4/(4\pi)^2)(v/M_S) \sin 2\beta$, which is negligible in comparison with $\lambda_{\text{eff}}^{\text{tree}}$.
 [35] J. Cao, F. Ding, C. Han, J. M. Yang, and J. Zhu, *J. High Energy Phys.* **11** (2013) 018.
 [36] J. Baron *et al.* (ACME Collaboration), *Science* **343**, 269 (2014).
 [37] Y. Sakemi *et al.*, *J. Phys. Conf. Ser.* **302**, 012051 (2011).
 [38] D. Kawall, *J. Phys. Conf. Ser.* **295**, 012031 (2011).
 [39] D. M. Kara, I. J. Smallman, J. J. Hudson, B. E. Sauer, M. R. Tarbutt, and E. A. Hinds, *New J. Phys.* **14**, 103051 (2012).